Relaxed Static Stability Aircraft Design via Longitudinal Control-Configured MDO Methodology

Ruben E. Perez*, Hugh H. T. Liu†, and Kamran Behdinan‡

*,† Institute for Aerospace Studies, University of Toronto
4925 Dufferin Street, Toronto, ON, Canada, M3H 5T6
‡ Department of Aerospace Engineering, Ryerson University
350 Victoria Street Toronto, ON, Canada, M5B 2K3

Abstract

This paper describes a multidisciplinary design optimization (MDO) approach to the conceptual design of a commercial aircraft with relaxed static stability (RSS). Longitudinal flight dynamics analysis and control design are performed concurrently with other disciplinary analysis to augment and improve handling qualities. The developed methodology enables control-configured designs providing higher freedom of change at the conceptual design stage. A design example demonstrates the effectiveness of the proposed integrated approach to improve performance goals.

Keywords: Aircraft Design, Multidisciplinary Optimization, Flight Dynamics & Controls

Introduction

An alternative avenue to improve aircraft performance is by reducing the inherent static vehicle stability. Such reduction is frequently referred to as relaxed static stability (RSS) (Roberts et al., 1977). It allows for changing the size and weight of various aerodynamic surfaces, to improve the vehicle operational efficiency. The design of RSS aircraft has drawn attention in the academic and research communities since the 1970s (Holloway et al., 1970). On the one hand, the main benefits of RSS are reflected in the reduction of wetted area drag, trim drag, and tail weight. In a transport aircraft with conventional stability margins, the horizontal tail accounts for approximately 20 to 30 percent of the aircraft-lifting surface and about 2 percent of its empty weight (Kroo, 1991). Although

An early version of this manuscript was presented as Paper 228 at the CASI Conference on Aerospace Technology and Innovation, Aircraft Design & Development Symposium, Toronto, ON, April 26-27, 2005

*Ph.D. Candidate, rperez@utias.utoronto.ca

†Associate Professor, liu@utias.utoronto.ca

‡Associate Professor and Chair, kbehdina@acs.ryerson.ca

the total weight and drag of the tail is small, the effects on the longitudinal stability and trim have a significant impact on the aircraft performance and cost (Sliwa, 1980). A study performed to lower the static stability limits for an L-1011 aircraft showed a significant reduction of the original tail area in the order of 30 percent and two percent decrease in aerodynamic drag (Foss et al., 1977). Similar studies have shown the improvement in performance with fuel savings in the order of 4 percent for a small transport aircraft with relaxed stability, advanced materials, and a more efficient propulsion system (Williams, 1983). On the other hand, the relaxation of stability margins degrades the handling qualities of the aircraft. It requires dynamic stability compensation or augmentation from active flight controls. Considerations of dynamic characteristics and control design are in fact essential in the design of a RSS aircraft. However, explicit consideration of flight dynamics and control is traditionally taken into account after the aircraft geometric characteristics have been established, leading to sub-optimal designs with increased constraints imposed on control effectors (see e.g. Sahasrabudhe et al., 1997). The "classical" control surface sizing procedures at the conceptual design stage are limited to use historical trends of the *volume coefficient* (Nicolai, 1984). They do not consider or take advantage of the interactions between different disciplines and flight dynamics and controls for the RSS aircraft. This paper presents a methodology to the design of a relaxed static stability commercial aircraft configuration. It enables the simultaneous consideration of stability and control characteristics with other conceptual design disciplines using a multidisciplinary design optimization (MDO) paradigm (Perez et al., 2004). Specifically, the longitudinal flight dynamics and control (FD&C) is considered due to its strong impact on RSS. The proposed multidisciplinary integration enables control-configured vehicle design.

FD&C Integration Methodology

In this section the main challenges that limit the integration of FD&C in the conceptual design stage are discussed along with a solution methodology to overcome such challenges.

FD&C Integration Challenges

A series of challenges hinder the integration of FD&C in the conceptual design phase. They have led to the use of simple methodologies based on historical extrapolation of control surfaces characteristics. First of all, the aircraft design has to guarantee satisfactory flight characteristics over the entire flight envelope. This requires the flight dynamics analysis and control design along the flight envelope to ensure positive characteristics. Therefore, the challenge lies in how to define a minimum set of flight conditions that will ensure satisfactory flight characteristics over the entire flight envelope. Secondly, unlike many other disciplines involved in the design process, FD&C does not have an obvious figure-of-merit. A multitude of dynamic requirements, specifications, and constraints can be specified for the aircraft and its control system. The challenge lies in choosing the proper set of criteria to size the control surfaces. Thirdly, the control design process

is performed well into the preliminary design phases and is typically done in isolation. The challenge lies in how to enable control-configuration interactions at the conceptual design stage. A finally obstacle is how to deal with the increased data and computational complexity that arise when trying to overcome the above challenges.

FD&C Design-Constraining Flight Conditions

To overcome the first challenge, the critical flight conditions that are used for the sizing the control surfaces are identified. A set of analyses to be performed on those flight conditions are defined based on their interdisciplinary effect on the control surfaces sizing. Depending on the aircraft type and configuration characteristics, a specific set of flight conditions analyses will become critical imposing size constraint limits in the general configuration of the control surfaces and their respective effectors. Conditions for the design of longitudinal control effectors (which have the strongest effects for a relaxed static stability aircraft) are presented in Table 1. The table contains static, manoeuvre and dynamic considerations along the flight envelope.

Table 1: Longitudinal Design-Constraining Conditions

Control Effector Analysis	Applicable Flight Conditions	Critical CG Location	Applicable Requirement	Aircraft Configuration
1-g Trim	All	Fwd, Aft	FAR/JAR 25.161C	Dependent on Flight Condition
Approach 1-g Trim	Approach	Fwd	FAR/JAR 25.161C	Full Flaps
Landing 1-g Trim	Landing	Fwd	FAR/JAR 25.161C	Full Flaps, Landing Gear Down
Go-Around 1-g Trim	Climb	Aft	FAR/JAR 25.161C	Full Flaps, Landing Gear Down
Manoeuvre Load	All	Fwd	FAR/JAR 25.255	Dependent on Flight Condition
Go-Around manoeuvre	Approach	Fwd	FAR/JAR 25.255	Full Flaps
Rotation on Takeoff	Takeoff	Fwd	FAR/JAR 25.143	Takeoff Flaps, Landing Gear Down, in ground effect
Rotation on Landing	Landing	Aft	FAR/JAR 25.143	Full Flaps, Landing Gear Down, in ground effect
Dynamic Mode Oscillation	All	Fwd, Aft	FAR/JAR 25.181A	Dependent on Flight Condition

The first set refers to the critical static conditions. For longitudinal trim, the control effectors should maintain steady 1-g level flight so that forces and moments of the plane are balanced. This scenario becomes important at low speeds, in both fwd and aft cg limits. Special consideration of trim for the approach and go-around trim flight conditions is placed since they become critical with complex high lift devices where the aerodynamic pitching moment is large. Thus, it is highly demanding for the control effectors. The second set refers to the critical manoeuvre conditions where the control effectors should be able to achieve load factors between the maximum and minimum operational load factors. Typically, the manoeuvre load capability is checked with a pull-up from a dive over the flight envelope, this scenerio become critical with the maximum takeoff weight and fwd cg. One manoeuvre condition which requires special consideration, is the go-around manoeuvre capability. For this manoeuvre the control effectors should be able to provide 8 deg/sec^2 pitch acceleration starting from an approach trim condition. Takeoff rotation capability is analyzed with flaps, undercarriage extended, and in-ground effect. The aircraft control effectors should generate enough pitch moment to lift the nose wheel off the ground while providing 7 deg/sec^2 pitch acceleration for dry,

prepared runways. This scenario is most critical for maximum takeoff gross weight with the cg being located at its most fwd location. Similarly, the landing rotation (nose-down de-rotation) should be analyzed since it can become a critical condition on aircraft with complex high-lift systems and high c.g. locations. The final set takes into account critical dynamic characteristics where the dynamic mode response for both the un-augmented (open-loop) and augmented (closed loop) aircraft is assesed. With a control-augmented aircraft the closed-loop dynamic criteria assesment serves primarily for the evaluation of control laws. However, consideration of these conditions during the conceptual design stage ensures the aircraft is properly designed for adequate dynamic characteristics where control-augmentation is used to avoid excessive system demands. Note that many of the above critical conditions for the control effectors can be matched to the traditional design mission flight phases as specified for design towards performance; greatly simplifying the flight condition analyses.

FD&C Design Constraints and Requirements

A common metric for the above analyses is defined in terms of control power (control deflection) (Chudoba, 1996). Such deflections become FD&C disciplinary constraints, which should be met in order to ensure adequate flight control characteristics. The design goal of sizing and placing control surfaces is to provide sufficient, yet not excessive, control power to meet the requirements of the prescribed flight analyses. Additional dynamic response specifications for the aircraft, such as limits of oscillation, damping ratios, natural frequency requirements, and control force gradients, are defined based on military specifications (such as MIL-STD-1797 (1997)), or certification guidelines (such as FAR Parts 23 or 25.3).

In addition to the above specifications, control design requirements are defined to achieve internal stability of the control system, reject external disturbances, and assure adequate handling qualities (HQ) requirements. The assessment of HQ is closely related to dynamic considerations of the augmented closed-loop aircraft. Different handling qualities quantification procedures exist. For the longitudinal case the method such as the one proposed in Anon (1980) is very useful for an optimization procedure. It directly quantifies dynamic modes responses characteristics with HQ. For example, if the aircraft dynamics is considered to be uncoupled into longitudinal and lateral modes, the short period mode handling quality can be assessed by using a generic control anticipation parameter (GCAP). The GCAP is a modified version of the control anticipation parameter that is applicable to both un-augmented and control augmented aircraft Gautrey et al. (1998). The parameter is defined as:

$$\begin{aligned} &GCAP = \frac{\dot{q}(0)}{n_z(t_{pk})}\left(1+\exp\left(\frac{-\zeta_{sp}\pi}{\sqrt{1-\zeta_{sp}^2}}\right)\right) \\ &0<\zeta_{sp}<1 \end{aligned} \tag{1}$$

where $n_z(t_{pk})$ is the normal acceleration at the peak time in response to a control step input. Specified GCAP bounds correlate the qualitative HQ levels to the aircraft step

input dynamic response. In the case of the Phugoid mode, handling quality is related to the mode damping and time to double amplitude to ensure long enough time to stabilize the aircraft following a disturbance.

Multidisciplinary Design Integration

A multidisciplinary optimization (MDO) paradigm is used to overcome the computational complexity and disciplinary information challenge that arise with the FD&C formulation. It is possible with a MDO procedure to transform the traditional vertical design process into a horizontal process allowing concurrent consideration of disciplines and analyses. Among the different MDO strategies, Collaborative Optimization (CO) (Braun et al., 1996), Fig. 1, is one of the best alternatives to meet the functional requirements to integrate FD&C. CO is a bi-level optimization scheme that decouples the design process by providing the common design variables and disciplinary coupling interactions all at once in an upper level. This eliminates the need for an *a priori* process, where information is accumulated sequentially, to define the plant specification. Furthermore, it decomposes (decentralizes) the disciplines involved allowing independent local disciplinary optimizations which is advantageous for control design. When using local optimization schemes, the MDO mathematical foundation leads to a unique 'multidisciplinary feasible point', which is the optimal solution for all disciplines.

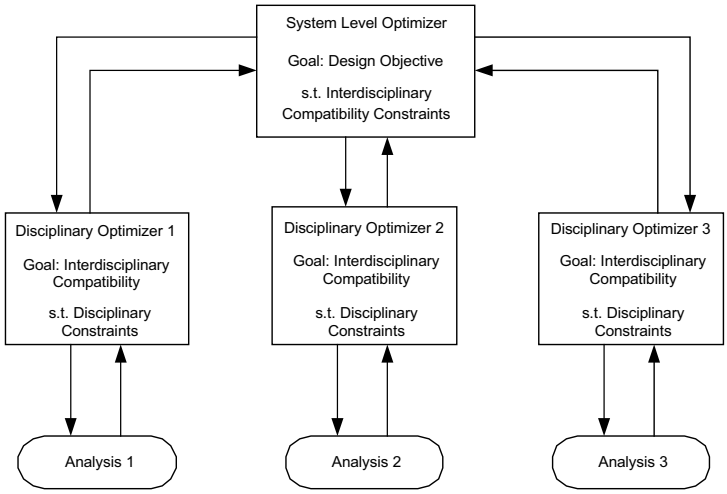

Fig. 1: Collaborative Optimization Method

At the system-level (SL), the Collaborative Optimization objective function is stated as:

$$\begin{aligned} &\min_{z_{SL},y_{SL}} \quad f\left(z_{SL},y_{SL}\right) \\ &s.t. \quad J_i\left(z_{SL},z_i^*,y_{SL},y_i^*\left(x_i^*,y_j^*,z_i^*\right)\right) \leq \varepsilon \quad i,j=1,...,n \quad j \neq i \end{aligned} \tag{2}$$

where f represents the system level objective function. J_i represents the compatibility constraint for the i^{th} subsystem (of the total n subsystems) optimization problem, and ε is a constraint tolerance value. Variables shared by all subsystems are defined as global variables (z). Variables calculated by a subsystem and required by another are defined as coupling variables (y), where y_i and y_j represent the i^{th} discipline output coupling and input coupling variables. Variables with superscript star indicate optimal values for the subsystem optimization, where z_i^*, y_i^*, and x_i^* are the i^{th} subsystem-optimal global, coupling, and local variables respectively. Note the system level constraint assures simultaneous coordination of the coupled disciplinary values.

The lower level objective function is formulated such that it minimizes the interdisciplinary discrepancy while meeting local disciplinary constraints. At the disciplinary level, the i^{th} subsystem optimization is stated as:

$$\begin{aligned} \min_{z_i, y_i, y_j, x_i} \quad & J_i\left(z_{SL_i}, z_i, y_{SL_i}, y_i\left(x_i, y_j, z_i\right)\right) = \sum\left(z_{SL_i} - z_i\right)^2 + \sum\left(y_{SL_i} - y_i\right)^2 \\ s.t. \quad & g_i\left(x_i, z_i, y_i\left(x_i, y_j, z_i\right)\right) \leq 0 \end{aligned} \tag{3}$$

where x_i are local disciplinary design variables, y_i are coupled disciplinary outputs state variables, y_j are coupled disciplinary input state variables, z_i are the system level variables required by the sub-system discipline analysis, and g_i is the specific disciplinary constraint.

From the above formulation, all required coupling information which forms the aircraft dynamic plant such as lift, drag, stability derivatives, and inertias, are provided to all disciplines simultaneously by the system level. Decomposition of the disciplinary analyses provides additional benefits in terms of control design and control-configuration integration in the design process. The local optimization variables x in (3) can be used as control design parameters to meet closed-loop specifications, while the z and y variables are used to achieve plant requirements.

Since the inclusion of dynamic analysis in the design process requires disciplinary analyses at different flight conditions, it increases the general problem complexity. However, we can take advantage of the MDO decomposition capabilities to analyze each discipline at each flight condition in a concurrent manner as shown in Fig. 3.

Control System Architecture

An important consideration is how to select or embody different control system architectures. Cook (Cook, 1999) states that unnecessary complication of the flight control system should be avoided. If there is no reason to complicate the flight control system design it should not be done. With this idea in mind, the initial goal when beginning the longitudinal flight control system design is aimed solely to increase the aircraft stability to meet close-loop and handling quality specifications. We define the aircraft plant as a strictly proper linear time invariant (LTI) system without disturbances and sensor noise as:

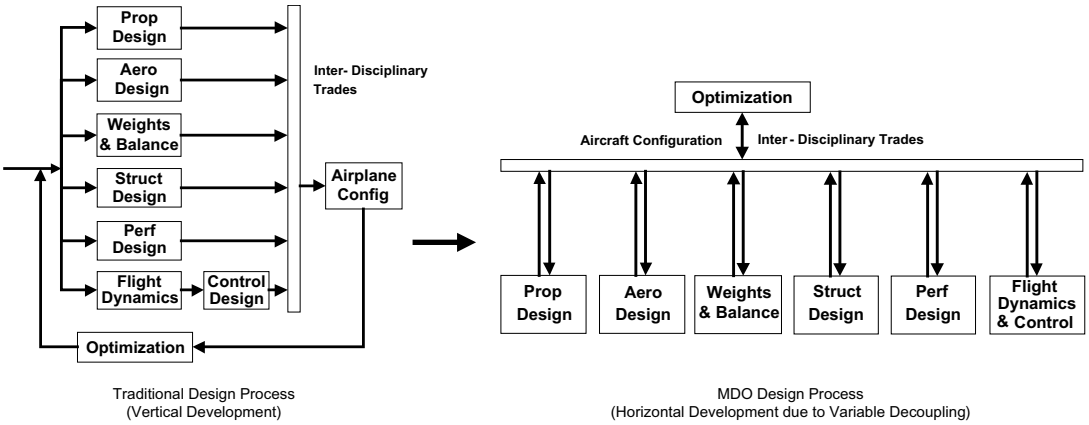

Fig. 2: Flight Dynamics and Control Decoupling

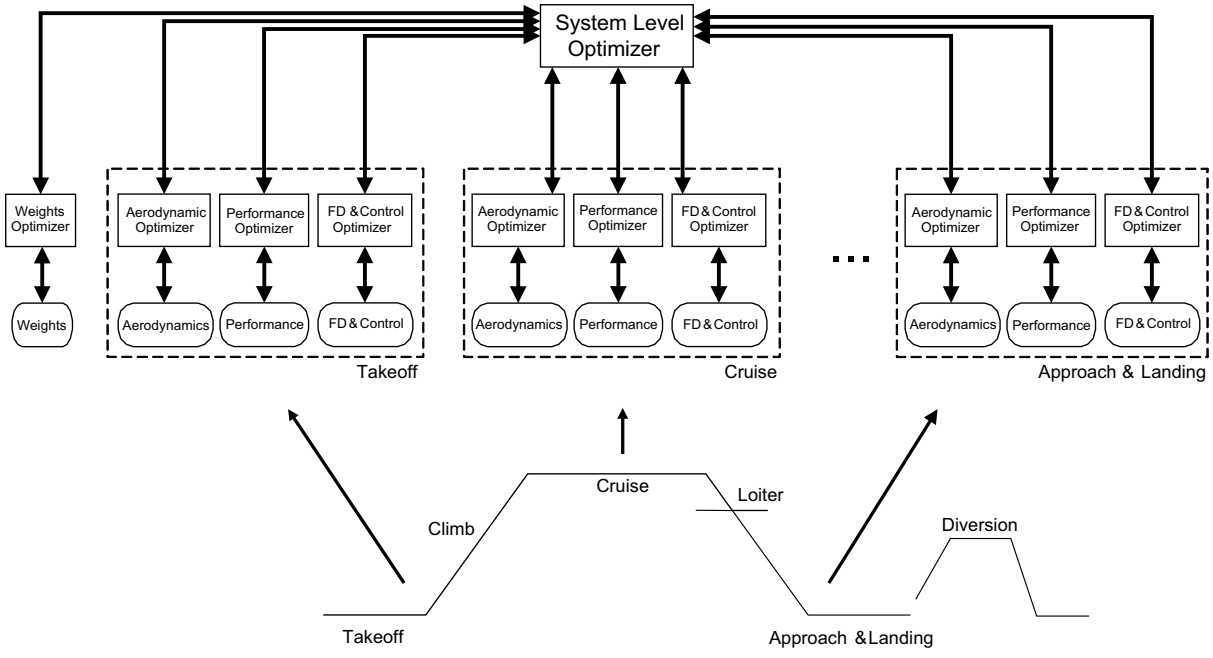

Fig. 3: Mission Segments Disciplinary Decomposition

$$\begin{aligned} \dot{x} &= Ax + Bu \\ y &= Cx \end{aligned} \tag{4}$$

where x is the aircraft states, y is the plant output, u is the control variables, and A, B, C are the state, control and output matrices respectively. An output feedback controller, Fig. 4, is used to provide the necessary stability augmentation. The feedback control is formulated as:

$$\begin{aligned} u &= r - Ky \\ where: \quad K &= \begin{bmatrix} k_{11} & \dots & k_{1d} \\ \vdots & \ddots & \vdots \\ k_{c1} & \dots & k_{cd} \end{bmatrix} \end{aligned} \tag{5}$$

where r is the reference control signal, c is the number of control variables u, and d is the number of state outputs y. Note that the above system can be fitted to handle single-input-single-output (SISO) or multiple-input-multiple-output (MIMO) control approaches providing a broader spectrum of control possibilities for the most demanding control tasks.

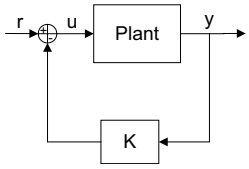

Fig. 4: Generalized Control Process

Application Example

Aircraft Mission and Optimization Goal

We can now illustrate the proposed integrated approach, in the case of a relaxed static stability 130-passenger, conventional aft tail, twin wing engine narrow-body airliner with a mission profile as specified in Fig. 5. The design goal (MDO system level goal, eq. (2)) is to find a feasible aircraft that maximizes specific air range ($\max_{z_{SL}, y_{SL}} \; Range$) while meeting individual disciplinary requirements. The maximum takeoff weight ($MTOW$) is specified as 117360 lb, while the payload weight is specified as 32175 lb based on 130 passengers, crew of 2, and 5 attendants. The subsystem level disciplinary optimization process follow the formulation presented in eq. (3) above.

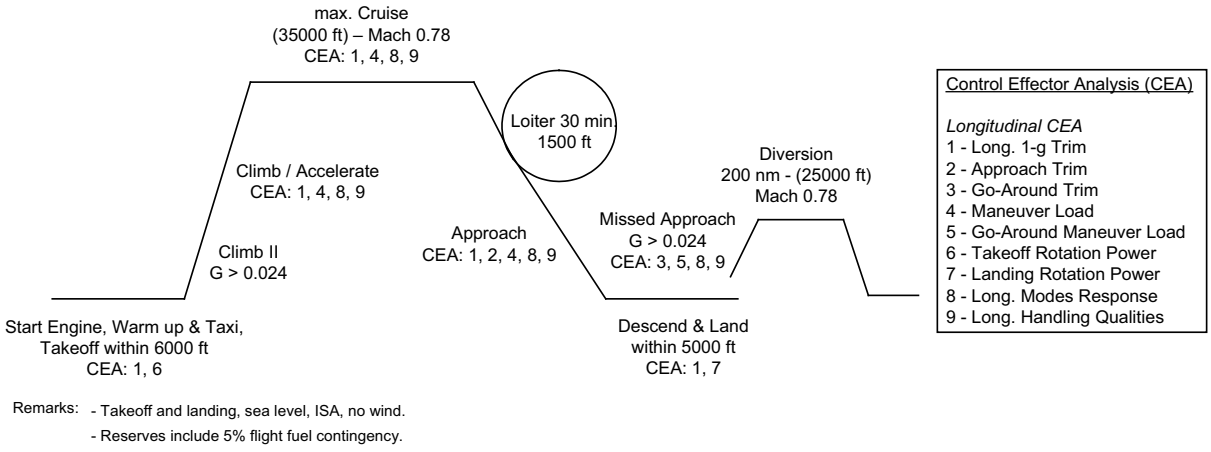

Fig. 5: Mission Profile and Longitudinal Control Effectors Analysis Considered

Disciplinary Analysis

The design process is composed of five coupled disciplines, namely: weights, aerodynamics, propulsion, performance, and dynamics & control, and are coupled as shown in the n-square diagram presented in Fig. 6. As shown in (3) the subsystem level objective is formulated to minimize the interdisciplinary discrepancies while meeting specific disciplinary constraints. Details of each discipline and specific constraints are described below.

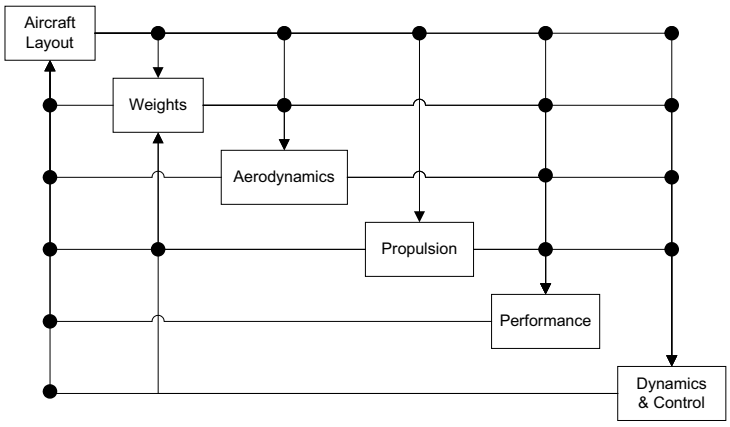

Fig. 6: Design Example Disciplinary Couplings

- Weights: The aircraft takeoff weight is calculated from main component weights that are estimated using statistical methods ((Torenbeek, 1990), (Raymer, 1999)). The maximum permissible center of gravity (cg) range for the configuration is calculated, from each aircraft component permissible cg limits based on their own geometry,

physical and functional considerations (Chai, 1995). Similarly, the aircraft inertias are calculated from a build-up based on each component inertias calculated from the mean c.g. location for each component.

- Aerodynamics: The general aerodynamic characteristics and stability derivatives are calculated in this discipline. Induced, parasite and wave drag calculations are considered. To provide greater flexibility and accuracy in the calculation of aerodynamic characteristics, semi-empirical models and a nonplanar, multiple lifting surface panel method are implemented. The induced drag is calculated from parametric technology models and the panel method. Parasite drag is calculated using a detailed component build-up (Roskam, 1998) taking into consideration viscous separation and components mutual interference effects. Transonic wave drag is modeled based on Lock's empirical approximation, using the Korn equation extended by Mason to include sweep (Malone et al., 1995). Downwash effects and stability derivatives are calculated from a combination of semi-empirical formulae ((Fink, 1975), (ESDU, 1987)) and lifting panel method results. The ground effect on induced drag has been taken into account using simplified empirical formulations such as those used in Hoerner et al., 1975, while the effect on lift and pitching moment characteristics has been taken into account using both a semi-empirical formulation as presented in Roskam, 1998, and a image mirror technique for the implemented panel method.

- Performance: Aircraft performance characteristics are analyzed for each flight mission segment as shown on Fig. 5. Field distances, rate of climb, and range are calculated based either on analytical expressions or numerical simulations. The landing field length is calculated assuming a landing weight of 90% MTOW. Specific air range is calculated based on the Breguet's equation, for the given aircraft total and fuel weights, lift and drag coefficients, specific fuel consumption, altitude and Mach number.

- Propulsion: Propulsion characteristics, such as engine weight, thrust and specific fuel consumption for a given altitude and Mach number, are calculated based on engine scaling of a baseline PW-2037 turbofan engine.

- Flight Dynamics and Control: It is assumed that all aircraft states are measurable without noise. Longitudinal design constraining, open-loop, and closed-loop analyses are performed at each flight mission segment as shown on Fig. 5. Control design is performed for all in-flight phases (climb, cruise, and landing approach) of the mission profile.

  Among the longitudinal modes the short period response is of prime concern due to its rapid response and its correlation with handling qualities evaluation. For this reason, we concentrate our efforts in the stability augmentation of this mode. The longitudinal short period flight dynamics equations can be formulated as:

$$\begin{bmatrix} \dot{\alpha} \\ \dot{q} \end{bmatrix} = \begin{bmatrix} Z_\alpha/V & 1 \\ M_\alpha + M_{\dot{\alpha}} Z_\alpha/V & M_q + M_{\dot{\alpha}} \end{bmatrix} \begin{bmatrix} \alpha \\ q \end{bmatrix} + \begin{bmatrix} Z_\alpha/V \\ M_\delta + M_{\dot{\alpha}} Z_\delta/V \end{bmatrix} [\delta_e] \quad (6)$$

where α is the aircraft angle of attack, q is the aircraft pitch rate, δ_e is the elevator deflection angle, V is the aircraft frestream velocity, and $[Z_\alpha, M_\alpha, M_{\dot{\alpha}}, M_q, Z_\delta, M_\delta]$ are dimentional stability derivatives. Note that every dynamic state is affected by the elevator deflection control input signal.

Control Systems Design

The control system considered consist of an output feedback controller, where the gains can be expressed as:

$$u = \delta_e = [k_\alpha, k_q] \begin{bmatrix} \alpha \\ q \end{bmatrix} \quad (7)$$

where stability of the closed loop system is guaranteed by selecting negative control gain values as seen in Fig. 7.

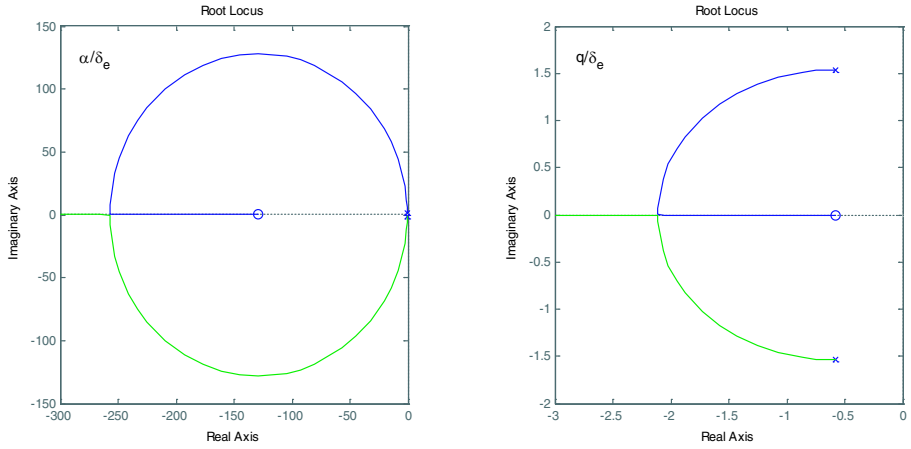

Fig. 7: Root Locus of the Closed Loop System

Design Variables

Table 2 lists the design variables, their bounds, and the initial design used in the optimization problem. Note that most of the coupling variables described will be repeated for each flight condition analyzed. At the system level, 61 design variables are taken into consideration, from which 19 are global design variables and 42 are coupling design variables. The global design variables include the main non-dimensional geometric variables which define the aircraft configuration. Coupling variables include 4 flight condition independent terms (engine scaling factor, MTOW, fuel and engine weights), while the rest are distributed over the different flight conditions. For example, 12 coupling

variables are shared by different disciplines for the cruise flight condition, namely: SFC, Thrust, CL_{max}, LD, CL and 7 stability derivatives. At the subsystem level, the total number of design variables depends on the specific disciplinary analysis considered and the analyzed flight condition. Local variables are specified only to the flight dynamic and control discipline and correspond to the longitudinal stability augmentation system design gains as described before. Additional required aircraft characteristics are provided as fixed parameters to the optimization problem. The nose gear location is assumed to be at 80% of the nose length: $xLG_{nose} = 0.8 * L_{nose}$. The main landing gear location is calculated assuming that 8% of the MTOW is applied on the forward wheels to provide sufficient weight on the nosewheel to permit acceptable traction for steering with the c.g. at its aft limit: $xLG_{main} = (xCG_{aft} - 0.08 * x_{nLG})/0.92$.

Table 2: Variables names, units, bound and initial design

Variable Name	Variable Type	Lower Bound	Upper Bound	Initial Design
Wing reference area (S_w), ft^2	Global	1000	1400	1200
Wing aspect ratio (AR_w)	Global	7	11	9
Wing taper ratio (λ_w)	Global	0.2	0.4	0.25
Wing LE sweep angle (Λ_w), deg	Global	25	35	30
Wing average thickness/chord ratio (tc_w)	Global	0.08	0.16	0.12
Wing location along fuselage ($xrLE_w$)	Global	0.25	0.5	0.4
Horizontal Tail area (S_{ht}), ft^2	Global	150	450	300
Horizontal Tail aspect ratio (AR_{ht})	Global	3	5	4
Horizontal Tail taper ration (λ_{ht})	Global	0.3	0.6	0.45
Horizontal Tail LE sweep angle (Λ_{ht}), deg	Global	25	45	35
Horizontal Tail thickness/chord ratio (tc_{ht})	Global	0.07	0.11	0.09
Vertical Tail area (S_{vt}), ft^2	Global	100	400	250
Vertical Tail aspect ratio (AR_{vt})	Global	1.4	1.8	1.6
Vertical Tail taper ratio (λ_{vt})	Global	0.3	0.6	0.45
Vertical Tail LE sweep angle (Λ_{vt}), deg	Global	25	45	35
Vertical Tail thickness/chord ratio (tc_{vt})	Global	0.09	0.12	0.11
Engine Scaling Factor (ESF)	Global	0.8	1.2	1
Maximum fuel weight (W_{fuel}), lb	Coupling	20000	30000	25000
Engine weight (W_{eng}), lb	Coupling	5664	8670	7160
Specific fuel consumption ($TSFC$), lb/hr/lb	Coupling	0.20	0.80	0.50
Engine Thrust (T), lb	Coupling	20000	35000	31000
Maximum Lift Coefficient (CL_{max})	Coupling	1.30	3.50	1.40
Lift to Drag Ratio (LD)	Coupling	6.00	25.00	10.00
Drag Coefficient (CD)	Coupling	0.01	0.50	0.25
Stability Derivative (Cz_a)	Coupling	1.00	20.00	10.00
Stability Derivative (Cm_a)	Coupling	-10.00	-0.10	-5.00
Stability Derivative (CL_q)	Coupling	1.00	20.00	10.00
Stability Derivative (Cm_q)	Coupling	-50.00	-0.10	-25.00
Stability Derivative ($Cm_{\dot{\alpha}}$)	Coupling	-50.00	-0.10	-25.00
Stability Derivative ($Cz_{\delta e}$)	Coupling	0.001	2.00	1.00
Stability Derivative ($Cm_{\delta e}$)	Coupling	-2.00	-0.001	-1.00
Control gain (K_a)	Local	-50.00	0.00	0.00
Control gain (K_q)	Local	-50.00	0.00	0.00

Design Constraints

The optimization constraints used at the subsystem level are shown in Table 3. They are split based on the analyze disciplines and flight phases. Geometric constraints are specified to meet airport handling requirements, by limiting the total wingspan, avoid flow separation at high Mach numbers, by restraining the sweep angle between the wing and the control surfaces, and assure the main landing gear can be mounted on the wing, by constraining the maximum permissible location of the gear with respect to the wing. Weight and balance constraints include the wing fuel space availability, as well as the maximum and minimum center of gravity limits for the aircraft. The aerodynamic constraints are specified to avoid negative aerodynamic compressibility effects, control re-

versal and flutter problems. Performance requirements constraints are specified based on Fig. 5 mission profile. The flight dynamic and control discipline include control power requirements as shown in Fig. 5, as well as flight condition dependent open and closed loop dynamic constraints. Note that the minimum level of static margin has been relaxed towards neutral stability, to take advantage of the reduced trim drag. We do not, however, allow for negative static margins, to comply with FAR 25.671 & 25.672 regulations. The longitudinal control effector area is defined to vary from 0.25 to 0.85 of the tail semi-span, with a uniform chord length of 30% the total tail chord. The maximum elevator control surface deflection limit is specified to ±25 degrees avoiding non-linear or undesirable aerodynamic behaviour of the flapped surface. Control power constraints deflection limits are allocated lower than the maximum allowed control effector deflection to provide allowance for additional control power requirements such as active control and turbulence disturbance rejection.

Table 3: Constraints for the Optimization Problem

Discipline	Flight Phase	Constraint Name	Value
Geometry	-	Wing span, ft	$\leq$ 260
Geometry	-	Wing LE sweep angle, deg	$\leq$ H.T. LE sweep angle
Geometry	-	Wing LE edge sweep angle, deg	$\leq$ V.T. LE edge sweep angle
Geometry	-	Main landing gear location, % MAC	$\leq$ 0.95
Weights	-	Avail. wing fuel volume, ft^3	$\leq$ Req. block fuel volume
Weights	-	Calculated MTOW, lb	= Specified MTOW
Weights	-	C.G. fwd position, % MAC	$\geq$ -0.15
Weights	-	C.G. aft position, % MAC	$\leq$ 0.65
Aerodynamics	Climb, Cruise, Approach, Go-Around	Wing Mach divergent drag number	$\geq$ Mach number
Aerodynamics	Climb, Cruise, Approach, Go-Around	H.T. Mach divergent drag number	$\geq$ Dive Mach number
Aerodynamics	Climb, Cruise, Approach, Go-Around	V.T. Mach divergent drag number	$\geq$ Dive Mach number
Performance	Takeoff	Takeoff field Length, ft	$\leq$ 5500. ft
Performance	Climb	Engine-out climb gradient	$\geq$ 0.024
Performance	Go-Around	Missed approach climb gradient	$\geq$ 0.024
Performance	Landing	Landing field Length, ft	$\leq$ 5000. ft
Propulsion	All Flight phases	Drag to Thrust Ratio	$\leq$ 0.88
FD&C	Climb, Cruise, Approach, Go-Around	Static Margin	$\geq$ 0.05
FD&C	Takeoff	Rotation elevator power, deg	$\leq$ 15
FD&C	Landing	Rotation elevator power, deg	$\leq$ 15
FD&C	Climb, Cruise, Approach, Go-Around	1-g Trim elevator power, deg	$\leq$ 15
FD&C	Climb, Cruise, Approach, Go-Around	Maneuver elevator power, deg	$\leq$ 15
FD&C	Climb, Cruise, Approach, Go-Around	Pitch - Vel. Axis Roll elevator power, deg	$\leq$ 15
FD&C	Climb, Cruise	Open-Loop short period damping ratio	$\geq$ 0.2, $\leq$ 2.0
FD&C	Approach, Go-Around	Open-Loop short period damping ratio	$\geq$ 0.35, $\leq$ 2.0
FD&C	Climb, Cruise, Approach, Go-Around	Open-Loop short period natural frequency	$\geq$ 1
FD&C	Climb, Cruise	Open-Loop short period GCAP for Level I handling quality	$\geq$ 0.038, $\leq$ 10
FD&C	Approach, Go-Around	Open-Loop short period GCAP for Level I handling quality	$\geq$ 0.096, $\leq$ 10
FD&C	Climb, Cruise	Closed-Loop short period damping ratio	$\geq$ 0.3, $\leq$ 2.0
FD&C	Approach, Go-Around	Closed-Loop short period damping ratio	$\geq$ 0.5, $\leq$ 1.3
FD&C	Climb, Cruise, Approach, Go-Around	Closed-Loop short period natural frequency	$\geq$ 1
FD&C	Climb, Cruise	Closed-Loop GCAP for Level I handling quality	$\geq$ 0.3, $\leq$ 3.3
FD&C	Approach, Go-Around	Closed-Loop GCAP for Level I handling quality	$\geq$ 0.16, $\leq$ 3.6
FD&C	Climb, Cruise, Approach, Go-Around	Closed-Loop System Eigenvalues	$\leq$ 0

Test Cases, Optimizer and Accurancy

Two illustrative cases are implemented to demonstrate the advantage of the proposed methodology. The first one optimizes the aircraft including FD&C considerations. The

second one performs a traditional conceptual design process without FD&C, where the horizontal tail area is constrainted using only the tail volume coefficient. To maintain uniformity, a Sequential Quadratic Programming (SQP) optimization algorithm (Nocedal, 1999) is used both at the system and the disciplinary levels. Proper scaling of the design variables, objectives and constraints is enforced for the gradient-based optimizer to handle discrepancies along the feasible/near-feasible descent direction when disciplines constraints force incompatibilities among the different subsystems. Due to the iterative nature of bi-level method, objective function gradients are evaluated using finite differences. Efficiency is measured based on the total number of disciplinary evaluations and the degree of interdisciplinary compatibility measured by the total discrepancy between each discipline optimum and the system level optimum. Tolerances for the optimization procedure where defined in the order of 10^{-6} based on initial studies to have a good compromise between the number of analysis calls at system and subsystem levels and the optimal objective function. Convergence of the optimization procedure is given when the search direction, maximum constraint violation and First-order optimality measure is less than a specified tolerance. By utilizing the SQP optimization, the multidisciplinary feasible optimum found will be a local optimum and will be dependent on the selected initial point.

Results

Optimized Designs and Comparisons

Table 4 shows the multidisciplinary feasible solution obtained from the integrated and traditional design test cases. The geometric configuration for both test cases is shown on Fig. 8. Both test cases meet the mission profile requirements and specified disciplinary constraints. An air-range improvement of 2% is obtained by the integrated FD&C control-configured design as compared to the traditional design approach. By simultaneously considering the aircraft dynamics and active stability control augmentation over the entire mission profile, a significant change in the aicraft configuration is achieved. The optimum aircraft layout comparison is shown as well in Fig. 9. The main difference is reflected in the horizontal tail area configuration and forward shift of wing apex. Both changes affect the center of gravity of the aircraft and reduce its static margin. At the same time, active control assures the required level of stability, to safely fly the aircraft, is achieved as will be shown below. The wing area is reduced 1.5% while the sweep angle is increased; this improves the aircraft pitch moment and produces more benign stall behaviour. However, the forward shift of the wing apex add to the main landing gear complexity in order to mount it to the wing. The horizontal tail area is reduced 28% as compared with the traditional design, while the aspect ratio decreases 39%. Lowering the aspect ratio proves beneficial for the configuration since it delays the stall angle of attack as compared with the traditional design and provides adequate control well after the wing has stalled. The tail sweep increases as well, avoiding flow separation at high Mach numbers and improving pitch moment characteristics.

Table 4: Traditional and Integrated FD&C Optimization Results

Variable Name	Traditional	Integrated FD&C
Wing reference area (S_w), ft^2	1176.48	1158.69
Wing aspect ratio (AR_w)	10.999	11.000
Wing taper ratio (λ_w)	0.221	0.200
Wing LE sweep angle (Λ_w), deg	29.11	34.92
Wing average thickness/chord ratio (tc_w)	0.122	0.117
Wing location along fuselage ($xrLE_w$)	0.350	0.283
Horizontal Tail area (S_{ht}), ft^2	287.08	205.71
Horizontal Tail aspect ratio (AR_{ht})	5.000	3.028
Horizontal Tail taper ratio (λ_{ht})	0.500	0.600
Horizontal Tail LE sweep angle (Λ_{ht}), deg	40.00	45.00
Horizontal Tail thickness/chord ratio (tc_{ht})	0.081	0.080
Vertical Tail area (S_{vt}), ft^2	257.79	231.03
Vertical Tail aspect ratio (AR_{vt})	1.600	1.610
Vertical Tail taper ratio (λ_{vt})	0.400	0.500
Vertical Tail LE sweep angle (Λ_{vt}), deg	45.00	45.00
Vertical Tail thickness/chord ratio (tc_{vt})	0.090	0.090
Engine Scaling Factor (ESF)	0.800	0.800
Maximum fuel weight (W_{fuel}), lb	30000	30000
Engine weight (W_{eng}), lb	5664	5664
Specific fuel consumption ($TSFC$) @ Cruise, lb/hr/lb	0.5034	0.5034
Engine Thrust (T) @ Takeoff, lb	25056	25056
Maximum Lift Coefficient (CL_{max}) @ Takeoff	2.51	2.42
Maximum Lift Coefficient (CL_{max}) @ Cruise	1.50	1.42
Maximum Lift Coefficient (CL_{max}) @ Cruise	3.10	2.92
Lift to Drag Ratio (LD) @ Cruise	18.373	18.789
Drag Coefficient (CD) @ Cruise	0.023	0.023
Lift to Drag Ratio (LD) @ Approach	9.999	9.695
Drag Coefficient (CD) @ Approach	0.188	0.179
Lift to Drag Ratio (LD) @ Climb	9.591	9.327
Drag Coefficient (CD) @ Climb	0.181	0.180
Maximum takeoff weight ($MTOW$), lb	117360	117360
Payload Weight (W_{pay}), lb	32175	32175
Range, nm	4238	4334
Takeoff Field Length, ft	4861	5105
Landing Field Length, ft	4301	4423
Engine-out climb gradient	0.067	0.068
Missed approach climb gradient	0.087	0.086
Wing Mach divergent drag number @ Cruise	0.7827	0.7991
Horizontal Tail divergent drag number @ Cruise	0.8469	0.8600
Vertical Tail divergent drag number @ Cruise	0.8260	0.8286

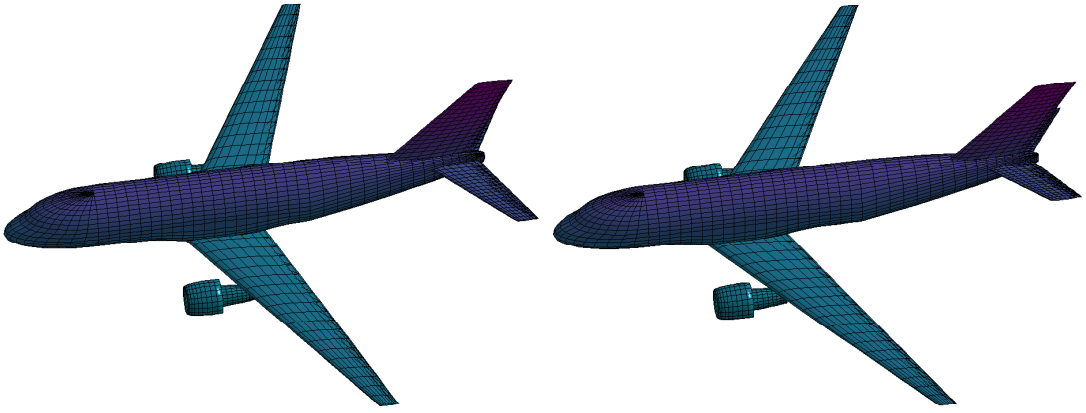

(a) Traditional Design (b) Integrated FD&C Design

Fig. 8: Test Cases Optimal Configurations

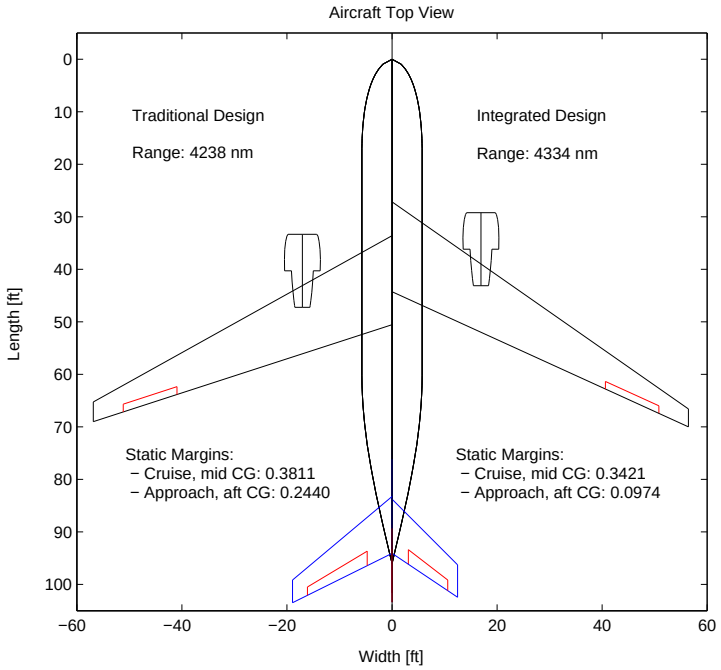

Fig. 9: Aircraft Configuration Comparison

Table 5 shows a comparison of the control power requirements between the two design cases. The integrated design shows reduced static margins; they originate from the horizontal area reduction and wing placement location. As expected, a larger elevator control deflection is required for takeoff rotation; this is however, within the limits of the specified deflection constraint. Other control power requirements are met with values lower than the specified limits; this provides ample margin of safety to deal with external disturbance rejection, or to cope with an increased control effort due to failures.

Table 5: Control Power and Open-Loop Dynamic Properties Comparison

Parameter	Traditional	Integrated FD&C
Static Margin @ Cruise, Mid CG	0.3811	0.3421
Static Margin @ Cruise, Aft CG	0.2025	0.1050
Static Margin @ Approach, Fwd CG	0.5592	0.5143
Static Margin @ Approach, Aft CG	0.2440	0.0974
Static Margin @ Climb, Fwd CG	0.5991	0.5143
Static Margin @ Climb, Aft CG	0.2438	0.0981
Takeoff Rotation elevator power, deg	-6.90	-11.14
1-g Trim elevator power, deg @ Cruise	5.37	6.26
1-g Trim elevator power, deg @ Approach	9.95	10.22
1-g Trim elevator power, deg @ Climb	12.56	12.03
Maneuver elevator power, deg @ Cruise	-10.53	-11.67
Pitch - Vel. Axis Roll elevator power, deg @ Cruise	1.91	3.17
Pitch - Vel. Axis Roll elevator power, deg @ Approach	3.80	6.16
Pitch - Vel. Axis Roll elevator power, deg @ Climb	4.04	6.24
Open-Loop short period damping ratio @ Cruise	0.2764	0.2519
Open-Loop short period damping ratio @ Approach	0.5234	0.5473
Open-Loop short period damping ratio @ Climb	0.3815	0.3497
Open-Loop short period natural frequency @ Cruise	2.4526	2.1558
Open-Loop short period natural frequency @ Approach	1.5369	1.2540
Open-Loop short period natural frequency @ Climb	2.0904	1.8891
Open-Loop short period GCAP @ Cruise	0.5538	0.4821
Open-Loop short period GCAP @ Approach	0.4037	0.2616
Open-Loop short period GCAP @ Climb	0.9665	0.783

RSS Design Dynamic Behaviour

Table 6 shows the optimal control gains and closed-loop characteristics of the integrated FD&C RSS design at different flight conditions. As before, we can see the found optimal design meet the specified closed-loop dynamic requirements and the stability augmentation gains are within acceptable limits and stabilize the short-period aircraft dynamics.

Table 6: RSS Design Closed-Loop Characteristics

Parameter	Cruise	Approach	Climb
Control gain (K_a)	-1.01	-0.010	-0.021
Control gain (K_q)	-0.98	-0.010	-0.015
Closed-Loop short period damping ratio	0.5365	0.5484	0.3515
Closed-Loop short period natural frequency	2.6883	1.2601	1.8928
Closed-Loop short period GCAP	0.729965	0.2589	0.7439
Short Period Eigenvalues	-1.4421 + 2.2687i	-0.6910 + 1.0538i	-0.6653 + 1.7721i

Typical flight characteristics of the RSS aircraft are demonstrated using a simulation of the aircraft dynamics for cruise and landing approach representative conditions. Longitudinal dynamic characteristics are shown on Fig. 10 and Fig. 11 for the cruise and approach flight phases respectively. On both flight phases the aircraft shows Level I handling quality with the stability augmented system as shown on Fig. 10(a) and Fig. 10(b). The response to an elevator step input by the augmented system is adequate, with a rapid disturbance rejection as shown in Fig. 10(b) and Fig. 11(b). The closed-loop dynamic behaviour in other flight conditions follow a similar behaviour to the one presented for the cruise and landing conditions.

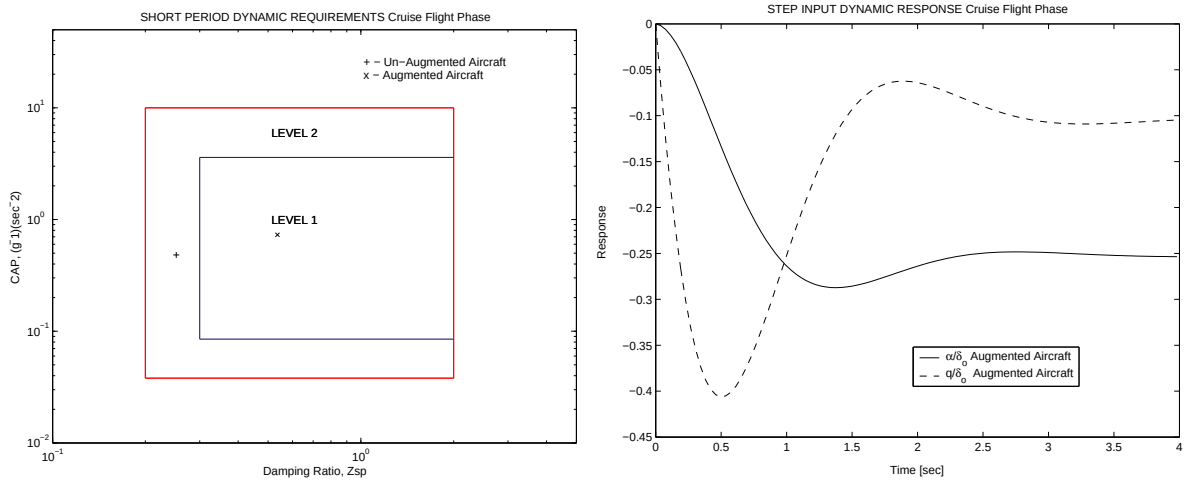

(a) Short-Period Handling Qualities

(b) Closed-Loop Response to Control Step

Fig. 10: RSS Design Cruise Longitudinal Dynamics Characteristics

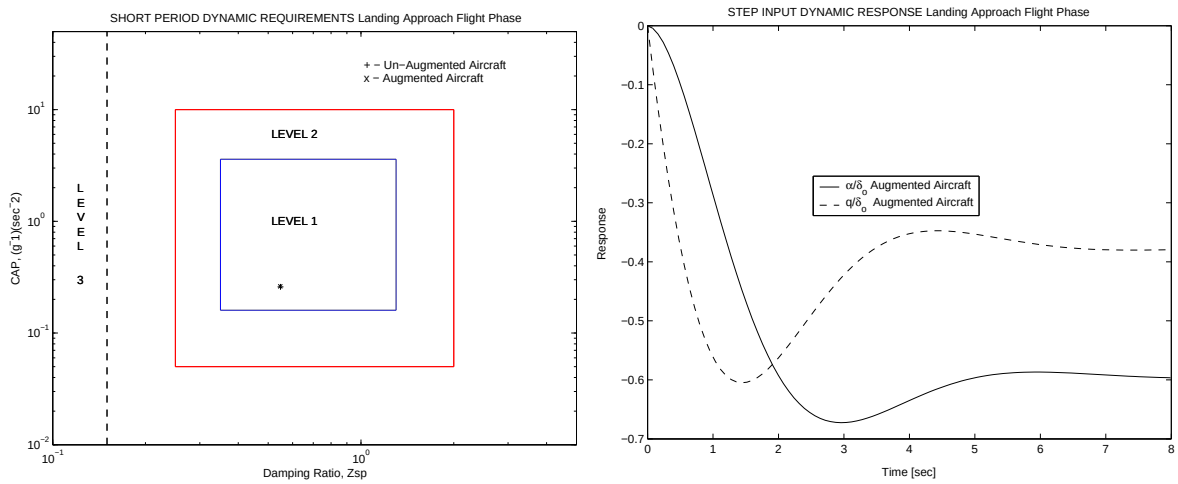

(a) Short-Period Handling Qualities

(b) Closed-Loop Response to Control Step

Fig. 11: RSS Design Landing Approach Longitudinal Dynamics Characteristics

Conclusion

The objective of this research was to determine the feasibility of integrating longitudinal flight dynamics and control at the aircraft conceptual design stage towards the design of a relaxed static stability aircraft. A methodology to overcome the difficulties arising from such integration was developed based on a multidisciplinary design optimization approach. It enabled longitudinal control-configuration considerations in the conceptual design process. Compared with other MDO aircraft design efforts, the integration of flight dynamics and control design requires the analysis of the interacting disciplines at multiple points over the flight envelope. Application of the methodology to the design of a relaxed static stability commercial aircraft was successful in producing optimal solutions with better performance than the traditional design process. The consideration of FD&C as an integral part of the conceptual design process takes advantage of active control, leading to a significant alteration of the aircraft configuration. The implemented approach could prove useful when considering aircraft configuration where flight dynamics plays a pivotal role such as the case of fly-by-wire aircraft or where conflicting dynamic requirements exist, such as the given case of supersonic aircraft design. It assures, from the conceptual stage, compliance with flight dynamic requirements avoiding costly design modifications at latter stages of the product development.

Acknowledgements

The authors thank the anonymous reviewers and editors for their insightful comments and suggestions, which improved this paper.

References

Anon (1980), Flying Qualities of Piloted Airplanes, *MIL SPEC*, MIL-F-8785C, U.S. Government Printing Office, Washington, DC.

Braun, R., Gage, P., Kroo, I., and Sobieszczanski-Sobieski, J. (1996), Implementation and Performance Issues in Collaborative Optimization, *Proceedings 5th AIAA/USAF MDO symposium*, AIAA Paper 96-4017, Bellevue, WA.

Chai S., Crisafuli P., and Mason, W.H., Aircraft Center of Gravity Estimation in Conceptual Design, *In Proceedings of the 1st Aircraft Engineering, Technology, and Operations Congress*, AIAA Paper 95-3882, Los Angeles, CA, Sept. 19-21, 1995.

Chudoba, B. (1996), Stability & Control Aircraft Design and Test Condition Matrix, *Technical Report EF-039/96*, Daimler-Benz Aerospace Airbus.

Cook, M.V. (1999), On the Design of Command and Stability Augmentation Systems for Advanced Technology Aeroplanes, *Transactions of the Institute of Measurement and Control*, Vol. 21, No. 2-3, pp. 85-98.

ESDU, Introduction to Aerodynamic Derivatives Equations of Motion and Stability, Item No. 86021, Engineering Sciences Data Unit, ESDU International plc, London, 1987.

Fink, R.D. (1975), USAF Stability and Control DATCOM, Air Force Flight Dynamics Lab., Wright-Patterson AFB, OH.

Foss, R.L., Lewolt, J.G. (1977), Use of Active Controls for Fuel Conservation of Commercial Transports, AIAA Paper 77-1220, American Institute of Aeronautics and Astronautics, Washington DC.

Gautrey, J.E., Cook, M.V., and Bihrle, W.A. (1998), A Generic Control Anticipation Parameter for Aircraft Handling Qualities Evaluation, *The Aeronautical Journal*, Vol. 102, No. 1013, pp. 151-159.

Hoerner, S., and Borst, H. (1975), Fluid Dynamic Lift, Hoerner Fluid Dynamics, Bricktown, NJ.

Holloway R.H., and Burris P.M. (1970), Aircraft Performance Benefits from Modern Control Systems Technology, *Journal of Aircraft*, Vol. 7, No. 6, pp. 550-553.

Kroo, I. (1991), Tail Sizing for Fuel-Efficient Transport, *AIAA Aircraft Design, Systems, and Technology Meeting*, AIAA Paper 83-2476, Oct. 1983, reprinted in AIAA Perspectives in Aerospace Design, C. Newberry editor.

Malone, B., and Mason, W.H. (1995), Multidisciplinary Optimization in Aircraft Design Using Analytic Technology Models, *AIAA Journal of Aircraft*, Vol. 32, No. 2, pp. 431-438.

Nicolai, L.M. (1984), *Fundamentals of Aircraft Design*, Second Edition, METS Inc.

U.S. Military Handbook MIL-HDBK-1797, 19 December 1997

Nocedal J, and Wright S. (1999). *Numerical Optimization*, First Edition, Series in Operational Research, Springer-Verlag, New York.

Perez, R., Liu, H.T., and Behdinan, K. (2004), Early Aircraft and Control Design Integration through Multidisciplinary Optimization and Surrogate Models, AIAA Paper 2004-5356, *AIAA Guidance, Navigation, and Control Conference and Exhibit*, Providence, Rhode Island.

Raymer, D.P. (1999), *Aircraft Design: A Conceptual Approach*, Third Edition, American Institute of Aeronautics and Astronautics, Washington DC.

Roberts, P.A., Swaim, R.L., Schmidt, D.K., and Hinsdale, A.J. (1977), Effects of Control Laws and Relaxed Static Stability on Vertical Ride Quality of Flexible Aircraft, *NASA Contractor Report*, NASA CR-143843, National Aeronautics and Space Administration.

Roskam, J. (1998), *Airplane Design*, Volumes 1-8, DARC Corporation, Ottawa, KS.

Sahasrabudhe, V., Celi, R., and Tits, A.L. (1997), Integrated Rotor-Flight Control System Optimization with Aeroelastic and Handling Qualities Constraints, *AIAA Journal of Guidance, Control and Dynamics*, Vol. 20, No. 2, pp. 217-224.

Sliwa, S.M. (1980), Economic evaluation of flying-qualities design criteria for a transport configured with relaxed static stability, *NASA Technical Publication*, NASA-TP-1980-1760, National Aeronautics and Space Administration.

Torenbeek E. (1990), *Synthesis of Subsonic Airplane Design*, Delft University Press and Kluwer Academic Publishers.

Williams, L. (1983), Small Transport Aircraft Technology, *NASA Special Publication*, NASA SP-0460, National Aeronautics and Space Administration.